1204–1212 Nucleic Acids Research, 1995, Vol. 23, No. 7 © 1995 Oxford University Press

Inhibition of HIV-1 reverse transcription by triple-helix forming oligonucleotides with viral RNA

Silke Volkmann, Jörg Jendis[2], Albrecht Frauendorf[1] and Karin Moelling*

Max-Planck-Institut für Molekulare Genetik, Abt. Schuster, Ihnestraße 73, D-14195 Berlin (Dahlem), Germany, [1]Institut für Organische Chemie, Johann Wolfgang-Goethe-Universität, Marie-Curie-Straße 11, D-60439 Frankfurt/Main, Germany and [2]Nationales Zentrum für Retroviren, BAG, Moussonstraße 13, CH-8028 Zürich, Switzerland

Received November 28, 1994; Revised and Accepted February 27, 1995

ABSTRACT

Reverse transcription of retroviral RNA into double-stranded DNA is catalyzed by reverse transcriptase (RT). A highly conserved polypurine tract (PPT) on the viral RNA serves as primer for plus-strand DNA synthesis and is a possible target for triple-helix formation. Triple-helix formation during reverse transcription involves either single-stranded RNA or an RNA•DNA hybrid. The effect of triple-helix formation on reverse transcription has been analyzed here *in vitro* using a three-strand-system consisting of an RNA•DNA hybrid and triplex-forming oligonucleotides (TFOs) consisting either of DNA or RNA. Three strand triple-helices inhibit RNase H cleavage of the PPT-RNA•DNA hybrid and initiation of plus-strand DNA synthesis *in vitro*. Triple-helix formation on a single-stranded RNA target has also been tested in a two-strand-system with TFOs comprising Watson–Crick and Hoogsteen base-pairing sequences, both targeted to the PPT-RNA, on a single strand connected by a linker $(T)_4$. TFOs prevent RNase H cleavage of the PPT-RNA and initiation of plus-strand DNA synthesis *in vitro*. In cell culture experiments one TFO is an efficient inhibitor of retrovirus replication, leading to a block of p24 synthesis and inhibition of syncytia formation in newly infected cells.

INTRODUCTION

The reverse transcriptase (RT) of HIV-1 catalyzes the conversion of viral RNA into double-stranded DNA (1,2). This process involves various steps, including initiation of RNA-directed DNA synthesis from a tRNA primer which continues after strand-switch to a full-length minus-strand DNA copy. The RNase H activity of the RT catalyzes the hydrolysis of the viral RNA in the RNA•DNA hybrid (3). Thereby a polypurine tract (PPT) is resistant to RNase H cleavage and serves as primer for plus-strand DNA synthesis by the DNA-directed DNA polymerase activity of the RT (Fig. 1). The PPT is a highly conserved region adjacent to the unique region at the 3′-end (U3) of the viral RNA in the coding region of the nef gene. A second PPT is located within the coding region of the integrase gene (4).

When considering approaches how to interfere with the viral life-cycle, we were attracted by the homopolymeric PPT because of its special and essential function during reverse transcription. A mutant in the RNase H domain of the RT, with an amino acid exchange in one of the most highly conserved amino acid residues H539N, exhibits a defect in its ability to initiate plus-strand DNA synthesis *in vitro* at the PPT-RNA primer level (5). This mutant construct when transfected into mammalian cells did not lead to infectious virus (6), proving that the mutation destroyed an essential viral function. Here, we tested whether the PPT can be masked as substrate for the RT by sequence-specific interaction with oligonucleotides. When the homopolymeric PPT functions as a target sequence, antisense oligonucleotides, as well as triple-helix-forming oligonucleotides (TFOs), might be useful tools to interfere with retroviral replication (7). Formation of a stable triple-helix with PPT *in vitro* has also been described previously for double- and single-stranded DNA targets (8–10).

It is postulated that during reverse transcription, TFOs targeted against single-stranded PPT-RNA or PPT-RNA•DNA hybrids might interfere at various points indicated by arrows and numbers in Figure 1. [1] At early stages of reverse transcription, DNA elongation during RNA-directed DNA synthesis might be arrested. [2] Hydrolysis of the RNA might be blocked at the PPT which prevents generation of a primer for plus-strand DNA synthesis. [3] Recognition of the 3′-end of the PPT-RNA during initiation of plus-strand DNA synthesis can potentially be inhibited. [4] Furthermore, the RNA-polymerase of the host cell can be blocked during transcription of double-stranded DNA to mRNA. [5] Finally, a triple-helix could also block translation of viral mRNA. The *in vitro* data presented here indicate that triple-helix formation is possible with a single-stranded RNA target as well as within an RNA•DNA hybrid region containing a PPT. We demonstrate that, in the presence of TFOs, essential steps of reverse transcription can be inhibited: the RNA-directed DNA synthesis, the generation of a PPT primer by the RNase H and the initiation of plus-strand DNA synthesis.

We designed and optimized the TFOs tested here with respect to their application in cell culture. Therefore, the TFOs were designed for an extended 25mer purine-rich target sequence, including the

* To whom correspondence should be addressed at present address; Institut für Medizinische Virologie, Universität Zürich, Gloriastrasse 30, CH-8028 Zürich, Switzerland

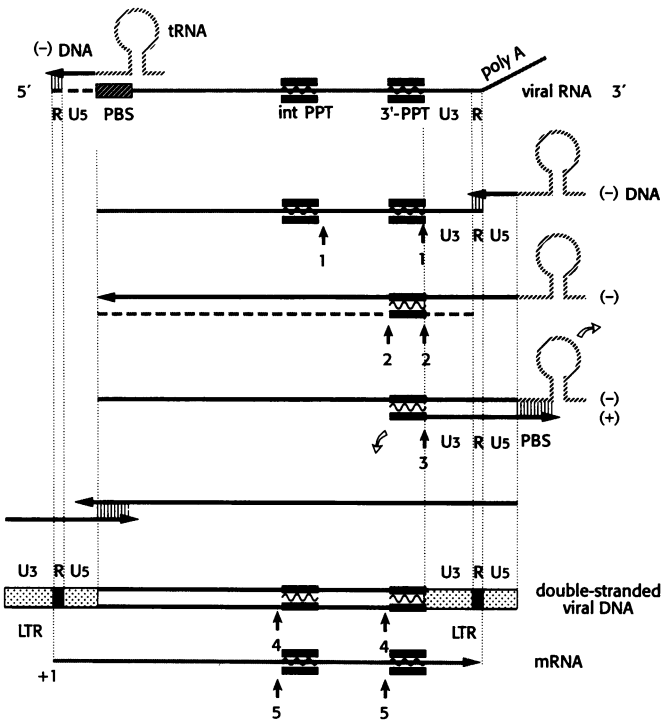

Figure 1. Model of the RT-catalyzed reverse transcription and the possible target-sites for triple-helix formation. The retroviral RNA genome contains two identical polypurine tracts (PPT) indicated by black bars. These polypurine sequences are potential target-sites for triple-helix formation which might interfere with reverse transcription at various steps. Reverse transcription of a poly(A) containing retroviral RNA genome initiates close to the 5'-end of the viral RNA at a tRNA primer which binds to a primer binding site (PBS). DNA synthesis continues at the 3'-end, whereby the two redundant regions R are involved. The reaction product of this minus-strand DNA synthesis is an RNA•DNA hybrid. The RNA moiety of this hybrid is hydrolyzed by the RNase H activity of the RT except for the PPT sequences which serve as primers for the plus-strand DNA synthesis. U_5 and U_3 indicate unique regions at the 5'- and 3'-ends, respectively. They become duplicated during double-stranded DNA formation and form the long terminal repeats, LTRs. Arrows and numbers point to events which might be inhibited by triple-helix formation: [1] inhibition of RNA-directed DNA synthesis; [2] inhibition of RNase H cleavage at the PPT which prevents the release of the primer for plus-strand DNA synthesis; [3] inhibition of initiation of plus-strand DNA synthesis; [4] inhibition of transcription of the double-stranded DNA provirus; [5] translation of the mRNA.

16mer PPT. The pyr•pur•pyr triple-helix type, which is highly pH-dependent and therefore not stable under physiological conditions, was avoided by a substitution of C^+ against G in the third Hoogsteen base-pairing strand. Additionally, the backbone composition (RNA or DNA) of the triple-helix was optimized.

Those TFOs which have been demonstrated to inhibit the action of the RT most effectively and form very stable triple-helices with the PPT-RNA *in vitro* were tested in cell culture experiments. One of them successfully abolished *de novo* infection of HIV-1.

MATERIALS AND METHODS

Oligonucleotides

Oligodeoxynucleotides (ODNs) were synthesized on an Applied Biosystems 380B synthesizer using standard phosphoramidate chemistry. Deprotection of the ODNs was achieved with aequeous ammonia. ODNs were purified by butanol precipitation and subsequently by HPLC prior to use. After butanol precipitation the oligoribonucleotides were purified via denaturing polyacrylamide gel electrophoreses or via HPLC. Chemicals used for oligonucleotide preparation were obtained from MWG-Biotech, Ebersberg, Germany and Peninsula, Merseyside, UK. Phosphorothioated ODNs were purchased from BioTez, Berlin, Germany. The oligoribonucleotides (ORNs) were obtained from TIP-Molbiol Co, Berlin.

T_m measurement

All T_m measurements were performed using a computer-controlled CARY 1 UV/VIS spectrophotometer (Varian) with temperature controller. Before the measurement, aliquots (2.5 µM) of target strand and TFO were dissolved in phosphate buffer (140 mM NaCl, 10 mM $MgCl_2$, 10 mM phosphate, pH 6.0). The samples were pre-denaturated at 85°C and slowly cooled to room temperature for re-annealing. The T_m curve was recorded at 260 nm with a temperature gradient of 0.5 K/min using our own software.

Expression and purification of HIV-1 RT

Expression and purification of the recombinant p66 wild-type and H539N mutant protein has been as described before (11,12). In a previous study the heterodimeric p66/51 RT has been tested in comparison to the homodimeric p66 HIV-1 RT (5). In various *in vitro* assays no difference in enzyme activity had been measured.

DNA manipulations

Restriction endonuclease cleavage, DNA isolation and end-labeling of DNA were performed as described by Maniatis *et al.* (13). *In vitro* transcription reactions were performed as described by the manufacturer (Stratagene). Sequencing reactions were carried out with a ^{32}P-end-labeled ODN primer using the dideoxy sequencing kit from USB according to the manufacturer's instructions. Construction of the plasmids pTZp8, pKJ11 and pKJ2 used for *in vitro* transcription reactions were as described before (14).

RNA•DNA hybrid formation

In vitro transcribed RNA harboring the PPT-target sequence was diluted in an association buffer consisting of 25 mM Tris–acetate, pH 6.8, containing 50 mM NaCl, 10 mM $MgCl_2$, 1 mM β-mercaptoethanol and 0.4 mM spermine hydrochloride, and incubated with a 3- or 10-fold molar excess of a complementary ODN for 3 min at 90°C, then cooled slowly to room temperature. These hybrids were either used directly as natural substrates for the RT or they were subsequently incubated overnight at 37°C with a TFO for analysing the possibility of triplex formation to interfere with RT functions.

RNase H cleavage protection assay

In vitro transcribed 5'-end-labeled pKJ2 RNA (7) was hybridized with a 40mer ODN complementary to the PPT region in the association buffer as described above. For triple-helix formation 20 nM RNA•DNA hybrid was incubated overnight at 37°C with increasing amount (200 nM, 500 nM, 2 µM, 5 µM, 10 µM and 20 µM) of the TF-ODN GT or the TF-ORN rGU. RNase H cleavage

reactions were performed in a total volume of 25 µl containing 12 ng RT as described before (7,14).

Inhibition of initiation of plus-strand DNA synthesis

Reactions with the natural RNA•DNA hybrid substrate were carried out as described using ^{32}P-end-labeled ODN N for the primer extension assay and the corresponding dideoxy sequencing reaction with plasmid pTZp8 (5,15). For triple-helix formation the RNA•DNA hybrid was incubated with a 100-fold molar excess of TF-ORN rGU (1 µM) overnight at 37°C. Enzyme reactions with the triple-helix substrate were carried out identically as described for the RNA•DNA hybrid substrate. Each assay was extracted with phenol, precipitated with ethanol and the pellet was resuspended in urea loading buffer (20 mM Tris–HCl, pH 7.4 containing 7 M urea, 10 mM EDTA, 0.5% SDS).

Triple-helix formation on a single-stranded RNA target

Analysis of RNase H cleavage protection were tested with *in vitro* transcribed 5′-end-labeled pKJ2 RNA. For triple-helix formation pKJ2 RNA (20 nM) was incubated with either 200 nM, 2 µM or 10 µM of TFO (A, B, C, D, E, F or—for control—KO A) in 20 µl association-buffer. The probes were incubated for 3 min at 90°C and then slowly cooled to 37°C. After overnight incubation at 37°C, a standard RNase H cleavage assay was undertaken as described above. To differentiate between a triplex effect or a direct RT inhibition, a primer-extension assay was performed using the various TFOs and a longer RNA [213 nucleotides (nt) designated pKJ11 in (5)]. A radioactive primer (5) binding downstream of the PPT was used to test cDNA synthesis with standard RT assay conditions (5).

Inhibition of HIV-1 replication in cell culture

Phosphorothioate oligodeoxynucleotides were tested for antiviral activity in a cellular acute infection assay. In this assay an HTLV-I transformed T-cell line C81-66/45 (16) was used (kindly provided by Dr R. C. Gallo, NCI, NIH, Laboratory of Tumor Cell Biology, Bethesda, MD, USA). The cell line was obtained after transformation of cord blood cells, co-cultivated with HTLV-I producing cells. The C81-66/45 cell line is non-productively infected with HTLV-I, since these cells do not express HTLV structural proteins p19 or p24 nor do they release detectable virus or reverse transcriptase activity into the culture medium (16).

To study the effect of the TFOs in cell culture the following TFOs were used: phosphorothioated TFO A (5′-TsTsTsTCTTTTGGGGGGTTTGGTTGGGsTsTsTsTCCCTTCCAGTCCCCCCTTTTCTsTsTsT), phosphorothioated TFO B (5′-TsGsTsGTGTGTGTGTGTGTGTGTGTGTsTsTsTsTTCCCTTCCAG TCCCCCCTTTTCTsTsTsT), a scrambled version of TFO A as control (5′-TsTsTsGGGGGGTTCTTCCTCTTTCCTTsTsTsTsTCGCCCGTCCGTTGCGTTGATTsTsTsT). Furthermore, a thioated 25mer antisense ODN (5′-CsCsCsTTCCAGTCCCCCCTTTTCTsTsTsT), corresponding to the Watson–Crick base-pairing sequence of the TFO A and B, and a scrambled derivative (5′-TsTsTsCCTTGATCCTCCTCTTCTTsCsTsT) were tested. Also the 2-*O*-methyl-derivative of rGU was used. HIV-1 replication was tested in short term experiments as described (17). 2×10^5 C81-66/45 cells per well of a 48 well plate were infected with 1 ml of HIV-1 type IIIB (18) containing supernatant which had been titrated for determination of infectivity. We used a low multiplicity of infection (moi ≈ 0.05). Viable cell number increased to 1×10^6 cells/ml within 4 days of incubation as determined by trypan blue exclusion. HIV-1 infection of these cells is characterized by the formation of large syncytia in culture which can be detected by microscope. Two hours after infection the cells were washed extensively and treated with the synthetic phosphorothioated oligodeoxynucleotides at 1 µM concentration in culture medium. After 48 h the medium was removed and fresh medium was added again containing the oligonucleotides at 1 µM concentration. Virus production was monitored at the cellular level by the appearance of syncytia and in the supernatants by p24 antigen-capture assay (Du Pont). At the time points indicated, an aliquot of the culture supernatant was removed for p24 antigen analysis and replaced by fresh medium. Once a week viable cells were counted and split down to 1×10^6 cells per ml. Short-term experiments were analyzed over a time period of 12 days. In the long-term experiment the effect of the TFO A in comparison to a corresponding 54mer random ODN on HIV-replication was analyzed over a time period of 28 days.

RESULTS

RNase H cleavage protection

The generation of the PPT-RNA primer for plus-strand DNA synthesis by the RT is an essential step during the process of reverse transcription (see Fig. 1). The RNA cleavage pattern of RNA•DNA hybrids containing *in vitro* transcribed RNA of the PPT region can be analyzed *in vitro*. These hybrids have been described before as substrates for the different RT activities (5,14). 85–90% of the RNA moiety of the hybrid were cut by the RNase H activity of the RT when the hybrid region is 20–40 bp in length (14).

In order to analyze whether triple-helix formation at the PPT can prevent RNase H cleavage at the 3′-end of the PPT-RNA, a preformed RNA•DNA hybrid consisting of a 40 bp hybrid region, including the extended PPT-target sequence was incubated with either a 25mer triplex-forming oligodeoxynucleotide GT (TF-ODN GT) or a 25mer triplex-forming oligoribonucleotide rGU (TF-ORN rGU) (Fig. 2A). In a previous study we have shown that under these conditions GT-containing TFOs prevent RNase H cleavage at the PPT more efficiently than their pyrimidine (CT-containing) counterparts (7). If the resistance against RNase H clevage is indeed caused by triplex formation, it should be further increased by changing the backbone composition of the triple-helix from D x R•D to R x R•D (x indicating Hoogsteen binding). This has been shown recently for pyr x pur•pyr triple helices (19,20).

Therefore we tested the effect of the TF-ORN rGU parallel to TF-ODN GT (Fig. 2B) under conditions (at pH 6.8) which should allow triple-helix formation and subsequent RT-treatment. While the presence of the TF-ODN leads to partial protection from RNase H cleavage, the TF-ORN rGU inhibits much more efficiently. The TFOs were tested over a range of concentrations starting with 20 nM causing no effect. At higher concentrations sequence specific RNase H cleavage protection is detectable. At the highest concentrations (>10 µM for rGU in lane 6, and >20 µM for GT in lane 7) direct enzyme inhibition is observed. This has been determined in a control experiment with a random hybrid substrate (data not shown).

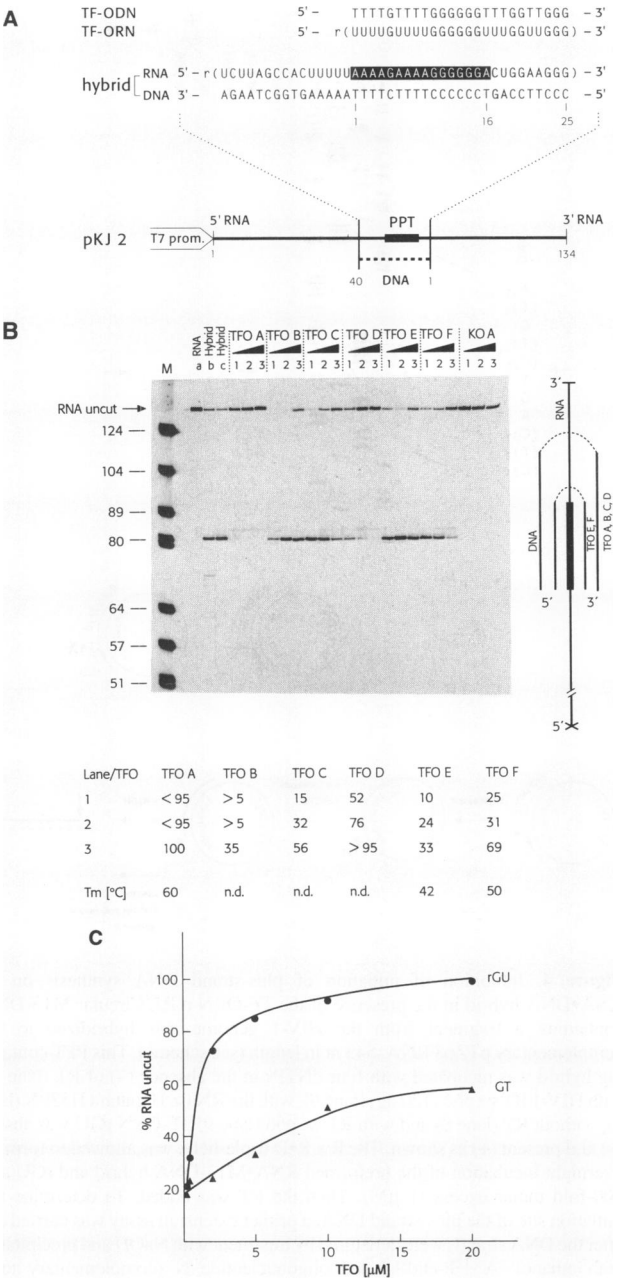

Lane/TFO	TFO A	TFO B	TFO C	TFO D	TFO E	TFO F
1	< 95	> 5	15	52	10	25
2	< 95	> 5	32	76	24	31
3	100	35	56	> 95	33	69
Tm [°C]	60	n.d.	n.d.	n.d.	42	50

Figure 2.(**A**) RNA•DNA hybrid (R•D) consisting of pKJ2 RNA (134 nt in length) was ^{32}P-end-labeled and hybridized to a 40mer ODN complementary to the PPT region indicated by dotted line. The sequence of the hybrid region is listed above. The PTT is marked as black bar in all figures. Two TFOs are shown on top, the TF-ODN GT and the TF-ORN rGU. (**B**) RNase H cleavage protection assay. A reaction mixture containing the RNA•DNA hybrid with 5′-end-labeled RNA (indicated by cross) was supplemented with increasing amounts of TF-ODN GT or TF-ORN rGU and incubated overnight at 37°C. RNase H was added for 30 min at 37°C and the RNA cleavage pattern analyzed on a denaturing 10% polyacrylamide gel, visualized by autoradiography and analyzed with a Phosphorimager (Molecular Dynamics). Lane a, control RNA alone; lane b, control without (–) RT; lane c, RNase H cleavage pattern of the RNA•DNA hybrid substrate (20 nM). Lanes 1–7, RNase H cleavage patterns obtained with RNA•DNA hybrid treated with increasing concentrations of either GT or rGU (20 nM, 200 nM, 500 ng, 2 μM, 5 μM, 10 μM and 20 μM). M, molecular weight marker, numbers refer to size of DNA fragments in base pairs. (**C**) Quantification of RNase H cleavage resistance in the presence of GT or rGU. The average amounts of uncut RNA from three independent RNase H cleavage assays were plotted against the concentrations of the TF-ODN GT or the TF-ORN rGU. Variations amount to 5–10%.

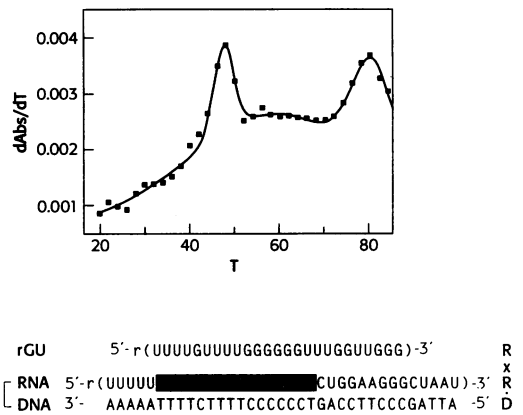

Figure 3. The optical melting curve of a simplified version of the R x R•D three-strand triple-helix system shown in Figure 2. Synthetic RNA including the PPT target sequence, a complementary oligodeoxynucleotide and the oligoribonucleotide rGU (all three as listed) were mixed with equimolar amounts and the T_m curve was recorded at 260 nm. The first derivative is plotted. The first transition at T_m 48°C corresponds to the dissociation of the triplex, the second transition at T_m 80°C to the disruption of the Watson–Crick RNA•DNA hybrid.

The data shown in Figure 2B were evaluated quantitatively by phosphorimager and the average of three experiments is presented (Fig. 2C). The TF-ORN rGU protects 50% of the RNA from cleavage at a concentration of ~1 μM whereas a 20-fold higher concentration of TF-ODN GT is required.

In order to confirm that the TF-ORN rGU can indeed form a triple-helix with the preformed hybrid, three strands consisting of a 35mer synthetic RNA oligonucleotide containing the extended PPT target sequence (listed at the bottom of Fig. 3), the complementary DNA oligonucleotide and the TF-ORN rGU, were subjected to an analysis of the UV absorbance at 260 nm as a function of temperature. The resulting melting profile presented in Figure 3 reveals two distinct peaks corresponding to transition from triplex to duplex at 48°C and transition from duplex to single-strands at 80°C. This result demonstrates that under the conditions tested a stable triple-helix formation is possible which can be assumed to cause RNase H cleavage protection at the PPT.

Inhibition of initiation of plus-strand DNA synthesis as a result of inhibition of the RNase H at the PPT

The presence of TF-ORN rGU can interfere with the RNase H activity at the PPT under conditions which allow triple-helix formation as shown above. On the basis of this result we anticipated that the initiation of plus-strand DNA synthesis might be inhibited. Therefore, the TF-ORN rGU was added to the RNA•DNA hybrid substrate at a concentration of 1 μM, which corresponds to a 100-fold molar excess over the preformed hybrid, and tested with purified RT *in vitro* the initiation of plus-strand DNA synthesis (5,15). For that purpose single-stranded circular phage M13 DNA containing an HIV-1 insert was hybridized to a complementary RNA (pT Zp8—543 nt in length) transcribed *in vitro* containing the PPT-target sequence (Fig. 4, see scheme at the bottom). The hybrid region is a substrate for the RNase H activity of the RT *in vitro*. In the presence of deoxynucleoside-triphosphates (dNTPs), the DNA-directed DNA polymerase activity of the RT initiates the synthesis of

DNA at the PPT, if the PPT becomes available as primer for initiation through action of the RNase H. After the RT has initiated DNA synthesis, the PPT•RNA primer should be removed. The 5′-end of the DNA initiated at the PPT can be mapped by primer extension from a primer annealed downstream. Such an assay was performed in the absence and presence of rGU. The result of a sequencing reaction is shown in Figure 4. Alignment of the result of the sequencing gel with the sequence listed to the left demonstrates that plus-strand DNA initiates exactly at the 3′-end of the PPT (arrows). When the TF-ORN rGU is added at a 100-fold molar excess to the preformed hybrid structure, initiation of DNA synthesis is inhibited (Fig. 4, lane 9). In a previous analysis we have demonstrated that a mutant of the RNase H with a point mutation H539N, which is defective in its exo- but not endonuclease function, cannot initiate plus-strand DNA synthesis in this assay (5) and is non-infectious (6). This result with the mutant and its respective wild-type is shown for comparison (Fig. 4, lanes 6 and 7). Two controls were performed with no enzyme present (lanes 5 and 8).

The data indicate that presence of the TF-ORN rGU prevents cleavage of the RNaseH activity at the PPT site so that initiation of plus-strand DNA synthesis is inhibited (indicated by crossed arrow in the scheme).

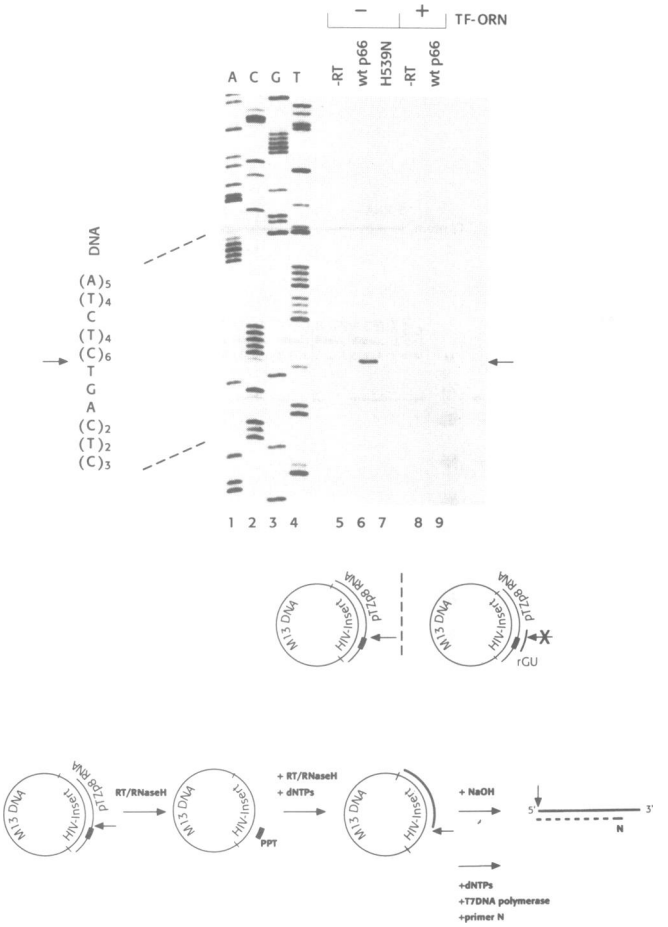

Figure 4. Inhibition of initiation of plus-strand DNA synthesis on an RNA•DNA hybrid in the presence of the TF-ORN rGU. Circular M13-DNA containing a fragment from the HIV-1 genome was hybridized to the complementary pTZp8 RNA, 543 nt in length (see scheme). This PPT-containing hybrid was incubated with four dNTPs in the absence (–) of RT (lane 5), with HIV-1 RT wt p66 (120 ng) (lane 6), with the RNase H mutant H539N (lane 7), without RT (lane 8) and with RT wt p66 (lane 9).TF-ORN rGU was absent (–) and present (+) as shown. The R x R•D triple-helix was allowed to form by overnight incubation of the preformed RNA•M13-DNA hybrid and rGU at a 100-fold molar excess (1 μM). Then the RT was added. To determine the initiation site of the plus-strand DNA, a primer extension assay was carried out after the DNA strands were denatured by treatment with NaOH and precipitated with ethanol. A ^{32}P-end-labeled oligonucleotide N (complementary to a sequence 66–86 bases downstream from the PPT, see scheme) was annealed to the plus-strand DNA and the primer extended up to the start point of plus-strand DNA synthesis by means of T7 DNA polymerase. The reaction products were applied to a denaturing 8% polyacrylamide gel along with dideoxy sequencing reaction ladders generated on the corresponding M13-DNA template with the unlabeled DNA primer N and [α-^{35}S]dATPαS (lanes 1–4) (Wöhrl and Moelling, 1990). The crossed arrow points to the inhibition site of the triple-helix.

RNase H cleavage protection in the presence of 'sandwich' TFOs

Triple-helix formation with an RNA target sequence can occur by preformation of an RNA•DNA duplex and the addition of a third Hoogsteen base-pairing strand. An alternative is a two-strand or 'sandwich' system consisting of a single-stranded RNA and a TFO which harbors the Watson–Crick and the Hoogsteen base-pairing sequence on a single strand separated by a linker sequence (21,22). This system is entropically and kinetically favoured and has been described before for the isomorphic (pyr x pur•pyr) triple-helix type with a single-stranded DNA containing the HIV-1 PPT as target sequence (21), not the viral RNA.

The *in vivo* target for a TFO is in the case of HIV-1 reverse transcription single-stranded RNA. Therefore, we determined whether such a sandwich TFO can interfere with enzyme activities of the RT especially the RNase H. Various TFOs were designed (listed in Fig. 5A) and RNase H cleavage assays were performed in their presence. *In vitro* transcribed RNA containing the extended PPT target sequence was preincubated with increasing amounts of the TFOs. All of these TFOs can form an RNA•DNA hybrid substrate for the RNase H activity with their Watson–Crick base-pairing sequence. The TFOs differ, however, in their Hoogsteen basepairing part where point-mutations were inserted. This influences their ability to form triple-helices. RNase H cleavage resistance was determined with radioactively 5′-end labeled RNA and analyzed by gel electrophoresis and autoradiography. Figure 5B shows the result of the RNase H cleavage reaction. Quantitative evaluation of the amount of RNA remaining uncut as measured by phosphorimager is presented below and given in percentage (Fig. 5B). Furthermore, spectroscopical analyses were performed to determine the triplex to duplex transition temperatures. T_m curves have been obtained with TFO A, E and F. T_ms of triplex to duplex transitions are listed (Fig. 5B, bottom). The sequence-specificity of the RNase H inhibition reaction is proven by TFO B which has a GT-alternating sequence in its Hoogsteen base-pairing part while its Watson–Crick base-pairing part was unchanged (see Fig. 5A). This TFOB which cannot form a triple-helix does not give rise to any RNase H cleavage resistance. Another control TFO contains a single mismatch in its Hoogsteen strand (TFO D). It still protects against RNase H cleavage. When, however, three mismatches were introduced into the Hoogsteen part (TFO C), a protection from RNase H cleavage is caused only at the highest concentration (10 μM). For comparison, triple-helix formation was analyzed with TFOs against the shorter PPT comprising only

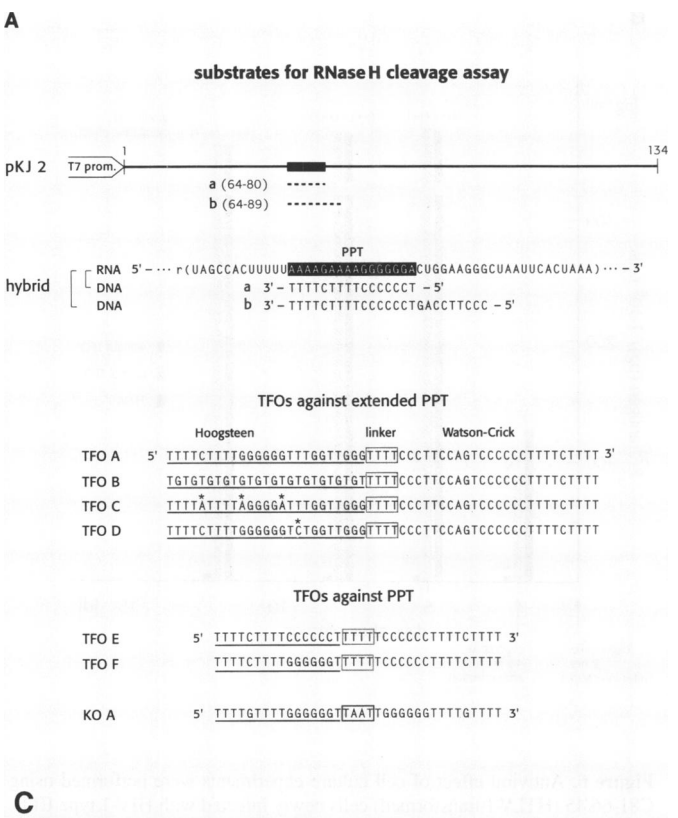

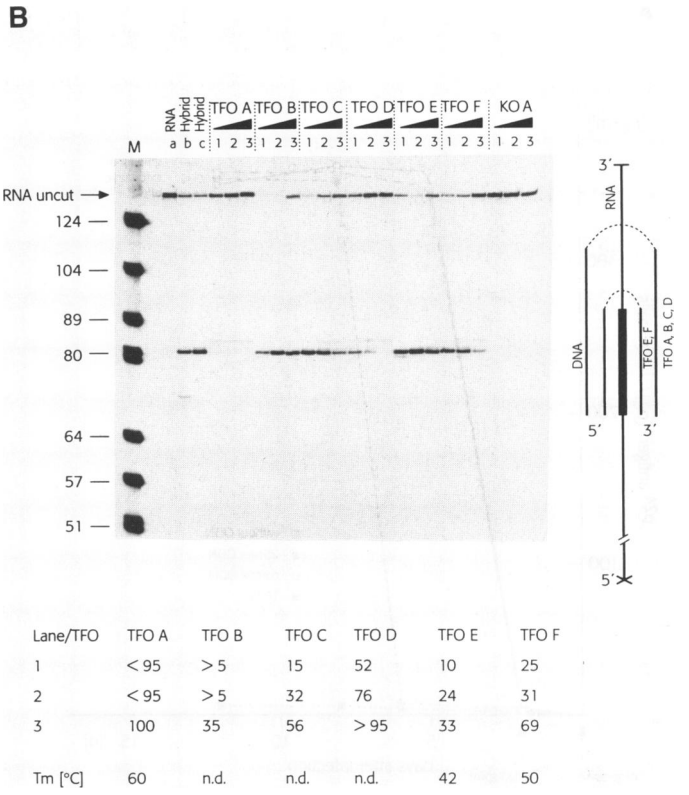

Lane/TFO	TFO A	TFO B	TFO C	TFO D	TFO E	TFO F
1	< 95	> 5	15	52	10	25
2	< 95	> 5	32	76	24	31
3	100	35	56	> 95	33	69
Tm [°C]	60	n.d.	n.d.	n.d.	42	50

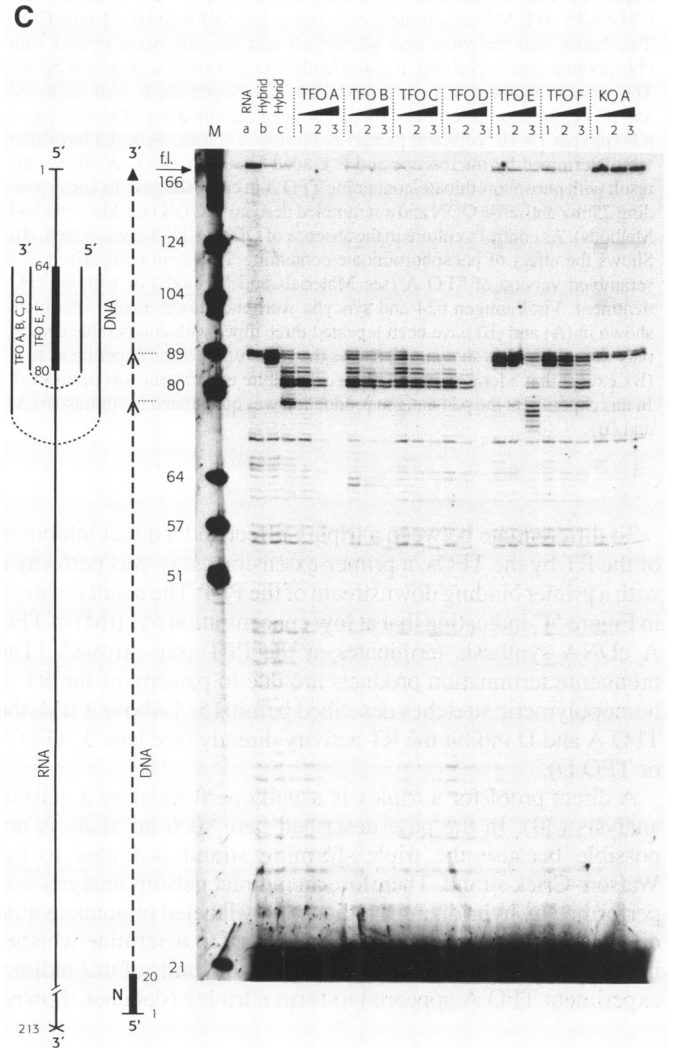

Figure 5. Analysis of RT activity in the presence of 'sandwich' TFOs. (**A**) Scheme of the natural RNA•DNA hybrid substrates consisting of pKJ2 RNA (134 nt) and the oligos a and b used for RNase H cleavage control reactions (top). Effect of triple-helix formation on single-stranded RNA target was tested with the TFO A through F and *in vitro* transcribed pKJ2 RNA. Stars indicate mutations, the box a T-linker. KOA is a control oligonucleotide which cannot form Watson–Crick base pairs with the target RNA. (**B**) RNA cleavage pattern in the presence of various TFOs. 5′-^{32}P-end-labeled pKJ2 RNA (20 nM) was treated with TFO A through F. Triple-helix formation was performed at 37°C overnight, then RT was added for 30 min at 37°C for RNase H cleavage assay. The reaction products were analyzed on a denaturing 10% polyacrylamide gel. Lane a, control with 5′-^{32}P-end-labeled pKJ2 RNA; lane b, RNase H cleavage patterns of the RNA•DNA hybrid pKJ2•a; lane c, RNase H cleavage pattern of the hybrid pKJ2•b. Lanes 1, 2 and 3, pKJ2 RNA (20 nM) with 200 nM, 2 μM and 10 μM of the TFOs as indicated. M, marker. The scheme to the right illustrates the expected triple-helix structures. Bottom: Quantification of the amounts of uncut RNA. In the presence of KO A the RNA was not cut and set to 100%. T_ms determined from spectroscopic measurements are listed at the bottom. nd indicates 'not determined'. (**C**) Primer extension assay in the presence of TFOs A–F. Lanes 1, 2 and 3 contain the TFOs as indicated at 200, 2 and 10 μM concentrations. Lane a, control primer extension with hybrid pKJ11 RNA (5), a longer version (213 nt) of pKJ2, and a radioactively labeled oligodeoxynucleotide primer N (5), which binds downstream of the PPT. Full-length (f.l.) and some shorter cDNA is synthesized (5). Lanes b and c, control reactions of primer extension with oligodeoxynucleotides corresponding to the Watson–Crick parts of TFO E–F and TFO A–D, respectively (i.e. control for an antisense effect). Faint bands originate from some pausing of RT at homopolymeric nucleotide stretches (5).

16 nt (for sequence see Fig. 5A). The GT-rich TFO F causes an RNase H cleavage protection effect only at its highest concentration (10 μM). In contrast, the pyrimidine containing TFO (TFO E) cannot protect the target RNA from RNase H cleavage. In summary, TFO-induced resistance against the RNase H shown in Figure 5B correlates well with the fidelity of the Hoogsteen binding third strand and the T_ms listed at the bottom.

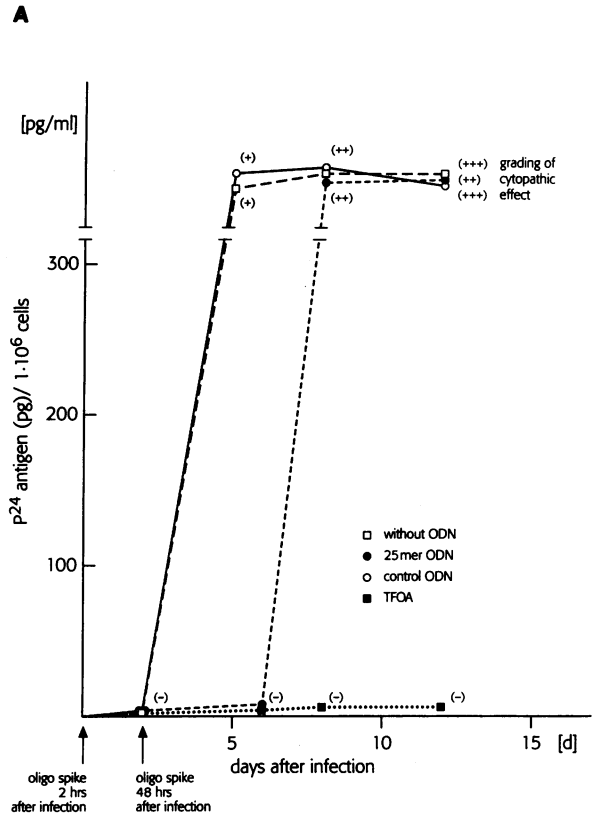

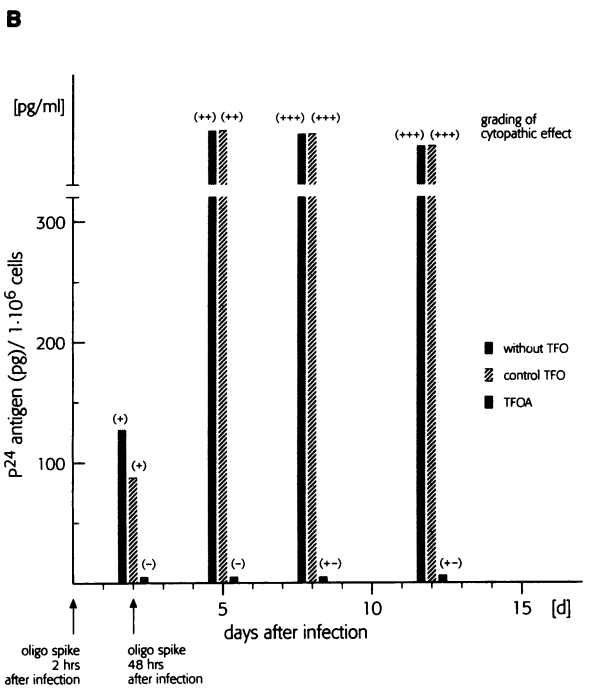

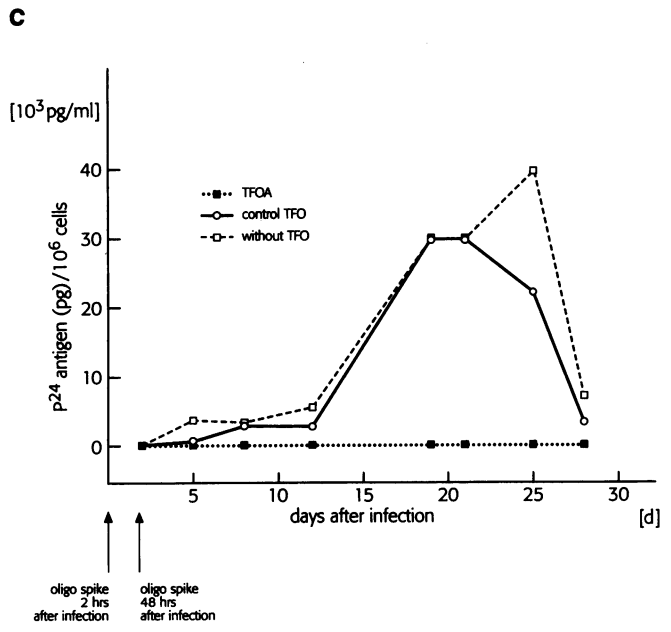

Figure 6. Antiviral effect of cell culture experiments were performed using C81-66/45 (HTLV-I-transformed) cells newly infected with HIV-1 type III B. Two hours later the virus was washed off and the cells were treated with phosphorothioate-containing oligonucleotides (1 μM each) as indicated below. The second treatment was performed 48 h later. Supernatants were collected and p24 expression determined by p24 antigen capture assay. The amount of p24 (pg) per 1×10^6 cells was plotted as a function of time. Syncytia formation was determined by microscope and is graded (–, +/– to +++). (**A**) shows the result with phosphorothioate-containing TFO A in comparison to its corresponding 25mer antisense ODN and a scrambled derivative ODN (see Materials and Methods). As control a culture in the absence of ODN or TFO A was tested. (**B**) Shows the effect of phosphorothioate-containing TFO A in comparison to a scrambled version of TFO A (see Materials and Methods) or without TFO treatment. Viral antigen p24 and syncytia were monitored. Each experiment shown in (A) and (B) have been repeated three times with comparable results, only one of which is shown. (**C**) shows the result of the same experiment as in (B), except that a long-term (28 days) cell culture experiment was performed. In this experiment the p24 antigen production was quantitated in contrast to (A) and (B).

To further characterize the reactions, an RNase H cleavage assay was performed with a hybrid region lacking the PPT sequence in the presence of increasing amounts of each TFO. As expected, the RNase H cleavage reaction was not inhibited. However, at higher concentrations (>1 μM) TFO A, and to a lesser extent TFO D, turned out to be inhibitory (data not shown), suggesting a direct effect on the enzyme. Thus, at higher concentrations of TFO A and D inhibition may result from a superposition of triple-helix formation and enzyme inhibition.

To differentiate between a triplex-effect and a direct inhibition of the RT by the TFOs, a primer-extension assay was performed with a primer binding downstream of the PPT. The result is shown in Figure 5C indicating that at low concentration (<1 μM) of TFO A cDNA synthesis terminates at the PPT (see arrows). [The premature termination products are due to pausing of the RT at homopolymeric stretches described before (5).] Above 1 μM, the TFO A and D inhibit the RT activity directly (see lane 3, TFO A or TFO D).

A direct proof for a triplex is usually performed by a gelshift analysis (30). In the case described here such an assay is not possible because the triplex-forming strand is linked to the Watson–Crick strand. Therefore an indirect gelshift analysis was performed by hybridizing a radioactively labeled oligonucleotide directed against the triplex-forming strand to determine whether it was bound to the target or not. Within the limits of this indirect experiment TFO A appeared to form a triplex (data not shown).

Effect of triple-helix forming oligonucleotideson HIV-1 replication in cell culture

To test the effect of inhibitory TFOs on replication of HIV in infected cells the most effective TFO A was chosen. Short-term experiments were performed similar to those described by Lisziewicz, for antisense effects on newly infected cells (17). The human T-cell line C81-66/45 was obtained by transformation of fresh human umbilical cord blood T-lymphocytes with HTLV-I (16). The immortalized cells contain the HTLV-I genome and synthesize viral RNA, but are restricted in their expression of viral structural proteins. These cells were acutely infected with HIV-1, strain IIIB. The amount of virus used for infection was determined beforehand by virus titration so that the infectious dose lead to syncytia within ~3 days. Cells were treated with virus for 2 h to allow adsorption. Then the virus was washed off and modified TFOs were added with fresh medium. After 48 h new medium supplemented with TFOs was added. At the time points indicated the amount of p24 in the supernatant was determined by p24 antigen capture assay (Du Pont) and plotted as a function of time (Fig. 6). Syncytia formation was determined by microscope and graded. The TFO A prevented syncytia formation and p24 production for up to 12 days. In this experiment a 25mer antisense ODN allowing Watson–Crick base-pairing in the PPT region (oligo b in Fig. 5A) and a control ODN consisting of randomized 25mer sequences were used as controls. Both ODNs contained three thioated nucleotides at either end (see Materials and Methods for sequences). The antisense ODN showed a transient inhibitory effect lasting for ~6 days whereas the control ODN had no effect (Fig. 6A). We also tested the effect of 2-*O*-methyl-derivative of TF-ORN rGU in such a short-term experiment. It did not exhibit any inhibitory effect on HIV replication (data not shown). The experiment shown in Figure 6A was repeated three times with similar results, one of which is shown.

In another experimental series TFO A was tested using the corresponding version of scrambled TFO A (see Materials and Methods) as control. Thioate modifications were again introduced in three nucleotides at either end and in three Ts of the T4 linker (see Materials and Methods). The result is shown in Figure 6B. It represents again one out of three experiments with similar results. A strong inhibition of virus replication as measured by p24 production, is observed, while the control did not have any effect.

Furthermore, we performed this experiment by extending the culturing period for up to 28 days (Fig. 6C). Again TFO A and the scrambled version of TFO A as control were used and each was applied twice as described above. The experiment shows complete inhibition of p24 antigen production in the presence of TFO A. In this experiment the amount of p24 production was quantitated in contrast to Figure 6A and B. The result shows that p24 production bursts off after 12 days in the controls (note differences in the scales in Figure 6A, B and C).

In another study TFO A was tested in comparison to TFO B. TFO B has a GT-alternating sequence in its 5′-part, which does not allow triple-helix formation. In cell culture TFO B had no effect on p24 or HIV-1 virus production (data not shown). This result demonstrates that the Watson–Crick base-pairing domain which could give rise to an antisense effect does not allow inhibition. Thus anti-sense effects can be excluded.

DISCUSSION

The PPT as a homopolymeric sequence has been tested for its ability to participate in triple-helix formation. The *in vivo* target for triple-helix formation during reverse transcription is, in the case of HIV, either single-stranded RNA or an RNA•DNA hybrid. Therefore, the inhibition of reverse transcription was tested *in vitro* using two model-systems. In the three-strand system a triplex-forming strand (TFO) was added to a preformed RNA•DNA hybrid. The second model-system consists of the single-stranded RNA target and a second oligonucleotide containing the Watson–Crick and the Hoogsteen base-pairing domains in a single strand separated by a spacer-sequence ('sandwich' or two-strand system).

The structure of the TFOs was designed for application in cell culture tests, which require high thermodynamic stability of the triple-helix, accessibility of the target for the TFOs and sufficient half-life of the TFOs to allow the slow process of triple-helix formation with the target strand before they degrade (23,24). The thermodynamic stability of a triple-helix depends on different factors such as length of the target sequence or backbone (RNA or DNA) and base-triplet composition (19,20,25–27). Consideration of these factors resulted in the design of the TF-ORN rGU for the three-strand system and TFO A for the two-strand system.

In vitro tests have confirmed the formation of a triple-helix with the PPT-RNA as target. Furthermore the presence of rGU leads *in vitro* to resistance of the PPT against RNase H cleavage and inhibition of initiation of plus-strand DNA synthesis. This defect has also been described previously (5) using the mutant RT, H539N, which did not lead to infectious virus when transfected into mammalian cells (6) proving that an essential viral function had been destroyed. Here, we demonstrate that an inhibitory effect of rGU on initiation of plus-strand DNA-synthesis occurs *in vitro*. However, in cell culture experiments the presence of rGU was unable to prevent *de novo* infection with HIV-1 (data not shown).

This result is consistent with other reports (27–29). In those studies a stable triple-helix formation can also be achieved *in vitro*. However, in cell culture experiments the triple helices were only effective when they were coupled with an intercalating agent such as psoralen and covalently linked to the target sequence by UV irradiation.

These chemical modifications of the Hoogsteen base-pairing triplex strand are one way to enable triple-helix formation under the high stringency of physiological conditions in living cells.

Here, another approach was taken. We analyzed whether the association of the Hoogsteen base-pairing triplex strand with the target strand can be facilitated if the Hoogsteen strand is covalently linked to a Watson–Crick base-pairing sequence. One of these 'sandwich' TFOs (TFO A), designed against single-stranded RNA, the *in vivo* target during HIV-1 replication, efficiently inhibits the RNase H activity *in vitro* and *de novo* infection in cell culture. In *in vitro* assays TFO A was shown to inhibit RNase H cleavage at the PPT-target site very efficiently even at low concentrations (200 nM) and the spectroscopical analysis proved a T_m for the triplex to duplex transition of 60°C when TFO A was annealed with single-stranded RNA as the target-strand. These results support the notion that a 'sandwich' composition of a triple-helix is thermodynamically and kinetically superior to the three-strand system. TFO A and, to a lesser

extent, TFO D inhibited the RNase H activity in a sequence-specific way, i.e. that a triplex really formed at the PPT and blocked the RNase H (Fig. 5B). This effect was not observed in a control reaction in which the TFOs were applied to a target-strand lacking the PPT. However, at higher concentrations (>1 μM TFO A) the RT/RNase H activities are directly inhibited as shown in a primer-extension experiment (Fig. 5C).

This raises the question of how TFO A inhibits retroviral replication in cell culture. We tried to exclude all obvious sequence-unspecific effects. The phosphorothioate-modified TFO A cannot interfere with retroviral binding at the CD4-receptor because the cells were incubated with infectious HIV-1 supernatant for 2 h before application of TFO A or the scrambled version of TFO A as control. A control without TFO or ODN demonstrated that under these conditions an HIV-1 infection was established and detectable within 3 days. Furthermore, a sequence-unspecific effect caused by the phosphorothioates can be excluded by the comparison of TFO A with the scrambled version of TFO A as control and TFO B. These two TFOs contain the same number of phosphorothioates at the analogous positions as TFO A, without having any effect on HIV-1 replication in cell culture assays. In the long-term experiment (28 days) we proved that the effect of TFO A is long-lasting. It can be excluded that the effect of TFO A is a simple antisense effect caused by its Watson–Crick base-pairing part. The effect of an antisense shown in Figure 6A is only a transient one. Furthermore, TFO B had no effect in tissue culture (not shown). TFO B is capable of forming Watson–Crick antisense structures but no triplex. Thus, we conclude, that the effect of TFO A in tissue culture is caused specifically by the structure of this compound. It is effective at 1 μM concentration in the culture medium which is very low compared to another intracellular triplex-study with the myc gene (31). Yet, this concentration is *in vitro* at the borderline between a triple-helix effect and a direct enzyme inhibition. A superposition of both may therefore play a role intracellularly. A structural analysis of TFO A suggests a hairpin-like stem–loop structure which is rather stable. It may mimic somehow the stacked bases of the PPT which represents a specific recognition site for the RT/RNase H. The TFO A may fit in between the two active centers of the RT and RNase H and functions as competitor of the PPT. The TFO A is G–C-rich and somehow reminiscent of the pseudoknot-forming structure determined as RT-inhibitor by Tuerk *et al.* (32) using the SELEX approach. The inhibitory effect of TFO A in cell culture is very stable which suggests that it prevents the establishment of infection. Whether it will be useful as antiviral agent needs to be investigated.

ACKNOWLEDGEMENTS

The excellent technical assistance of Rita Haubold and Dora Pontelli is gratefully acknowledged. The authors also thank Dr Zusanna Tomasik for performing the p24 antigen capture assays. We thank Dr Kyonggon Yoon, USA, for critical comments and helpful discussion. This work was supported by the Max-Planck-Society, the Deutsche Forschungsgemeinschaft, Swiss National Science Foundation and the BAG, Bern, to JJ.

REFERENCES

1 Baltimore, D. (1970). *Nature* **226**, 1209–1211.
2 Temin, H.M. and Mitzutami, S. (1970) *Nature*, **226**, 1211–1213.
3 Moelling, K., Bolognesi, D.P., Bauer, H., Büsen, W., Plassmann, H.W. and Hausen, P. (1971) *Nature New Biol.* **234**, 240–243.
4 Charneau, P., Alizon, M. and Clavel, F. (1992) *J. Virol,.* **60**, 2814–2820.
5 Wöhrl, B., Volkmann, S. and Moelling, K. (1991) *J. Mol. Biol.*, **220**, 801–818.
6 Tisdale, M., Schulze, T., Larder, B.A. and Moelling, K. (1991) *J. Gen. Virol.*, **72**, 59–66.
7 Volkmann, S., Dannull, J. and Moelling, K. (1993) *Biochimie*, **75**, 71–78.
8 Giovannangéli, C., Thuong, N.T. and Hélène, C. (1992) *Nucleic Acids Res.*, **20**, 4275–4281.
9 Giovannangéli, C., Rougée, M., Garestier, T., Thuong, N.T. and Hélène, C. (1992) *Proc. Natl. Acad. Sci. USA*, **89**, 8631–8635.
10 Sun, J.S., Giovannangéli, C., Francois, J.C., Kurfurst, R., Montenay-Garestier, T., Asseline, U., Saison-Behmoaras, T., Thuong, N.T. and Hélène, C. (1991) *Proc. Natl. Acad. Sci. USA*, **88**, 6023–6027.
11 Larder, B., Purifoy, D., Powell, K. and Darby, G. (1987) *EMBO J.*, **6**, 3133–3137.
12 Hansen, J., Schulze, T. and Moelling, K. (1987) *J. Biol. Chem.*, **262**, 12393–12396.
13 Maniatis, T. Fritsch, E.F. and Sambrook, J. (1982) *Molecular Cloning. A Laboratory Manual*, Cold Spring Harbor, NY.
14 Volkmann, S., Wöhrl, B., Tisdale, M. and Moelling, K. (1993) *J. Biol. Chem.*, **268**, 2674–2683.
15 Wöhrl, B. and Moelling, K. (1990) *Biochemistry*, **29**, 10141–10147.
16 Salahuddin, S.Z., Markham, P.D., Wong-Staal, F., Franchini, G., Kalyanaraman, V.S. and Gallo, R.C. (1983) *Virology*, **129**, 51–54.
17 Lisziewicz, J., Sun, D., Klotman, M., Agrawal, S., Zamecnik, P. and Gallo, R.C. (1992) *Proc. Natl. Acad. Sci. USA*, **89**, 11209–11213.
18 Popovic, M., Sarngadharan, M.G., Read, E. and Gallo, R.C. (1984) *Science*, **224**, 497–500.
19 Han, H. and Dervan, P.B. (1993) *Proc. Natl. Acad. Sci. USA*, **90**, 3806–3810.
20 Roberts, R.W. and Crothers, D.M. (1992) *Science*, **258**, 1463–1466.
21 Giovannangéli, C., Thuong, N.T. and Hélène, C. (1993) *Proc. Natl. Acad. Sci. USA*, **90**, 10013–10017.
22 Kool, E.T. (1991) *J. Am. Chem. Soc.*, **113**, 6265–6266.
23 Maher III, L.J., Wold, B. and Dervan, P.B. (1989) *Science*, **245**, 737–741.
24 Maher III, L.J., Dervan, P.B. and Wold, B.J. (1990) *Biochemistry*, **29**, 8820–8826.
25 Moser, H.E. and Dervan, P.B. (1987) *Science*, **238**, 645–650.
26 Griffin, L.C. and Dervan, P.B. (1989) *Science*, **245**, 967–971.
27 Young, S.L., Krawczyk, S.H., Matteucci, M.D. and Toole, J.J. (1991) *Proc. Natl. Acad. Sci. USA*, **88**, 10023–10026.
28 Grigoriev, M., Praseuth, D., Robin, P., Hemar, A., Saison-Behmoaras, T., Dautry-Varsat, A., Thuong, N.T., Hélène, C. and Harel-Bellan, A. (1992) *J. Biol. Chem.*, **267**, 3389–3395.
29 Grigoriev, M., Praseuth, D., Guieysse, A.L., Robin, P., Thuong, N.T., Hélène, C. and Harel-Bellan, A. (1993) *Proc. Natl. Acad. Sci. USA*, **90**, 3501–1505.
30 Yoon, K., Hobbs, C.A., Koch, J., Sardaro, M., Kutny, R. and Weis, A.L. (1992) *Proc. Natl. Acad. Sci. USA*, **89**, 3840–3844.
31 Postel, E.H., Flint, S.J., Kessler, D.J. and Hogan, M.E. (1991) *Proc. Natl. Acad. Sci. USA*, **88**, 8227–8231.
32 Tuerk, C., MacDougal, S. and Gold, L. (1992) *Proc. Natl. Acad. Sci. USA*, **89**, 6988–6992.